UNIMOLECULAR FRAGMENTATION INDUCED BY LOW ENERGY COLLISION: STATISTICAL OR DINAMICALLY DRIVEN?

Ana Martín-Sómer[1,2], Manuel Yáñez[1*], Marie-Pierre Gaigeot[2,3,4] and Riccardo Spezia[2,3*]

Contribution from [1]Departamento de Química, Facultad de Ciencias, Módulo 13. Universidad Autónoma de Madrid. Cantoblanco, 28049-Madrid. Spain, [2]Université d'Evry Val d'Essonne, UMR 8587 LAMBE, Boulevard F. Mitterrand, 91025 Evry Cedex, France, [3]CNRS, Laboratoire Analyse et Modélisation pour la Biologie et l'Environnement UMR 8587, France, and [4]Institut Universitaire de France (IUF).

Supporting Information
(15 pages)

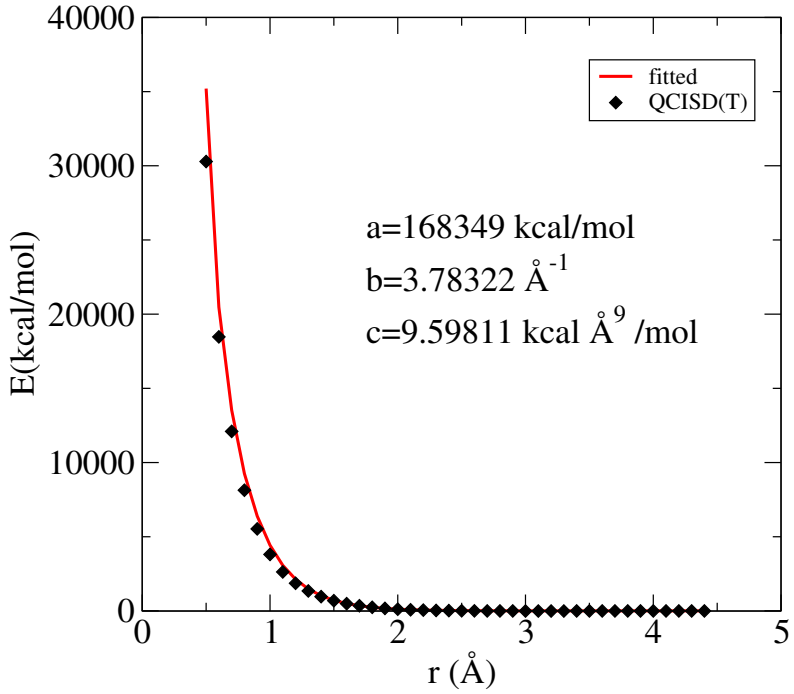

Figure S1: QCISD(T)/6-31++G(d,p) *ab initio* (diamonds) and fitted (solid line) potential energy curves for the Ar-Sr^{2+} interaction.

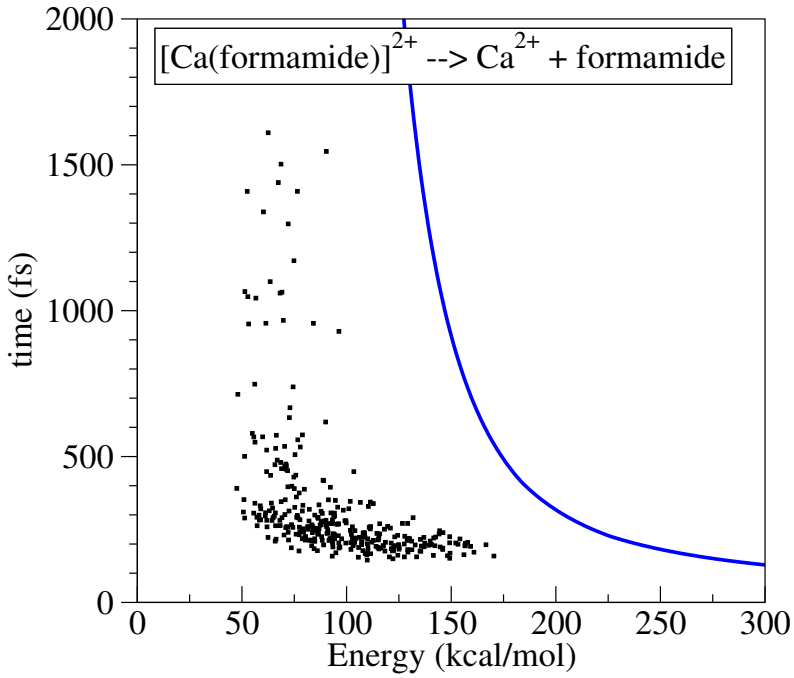

Figure S2: Reaction time *vs.* energy transfer for trajectories yielding formamide neutral loss, obtained from dynamics simulations (squares) and half life times ($t_{1/2}$) predicted by RRKM (solid line). Both were obtained using BLYP/6-31G(d) level of theory.

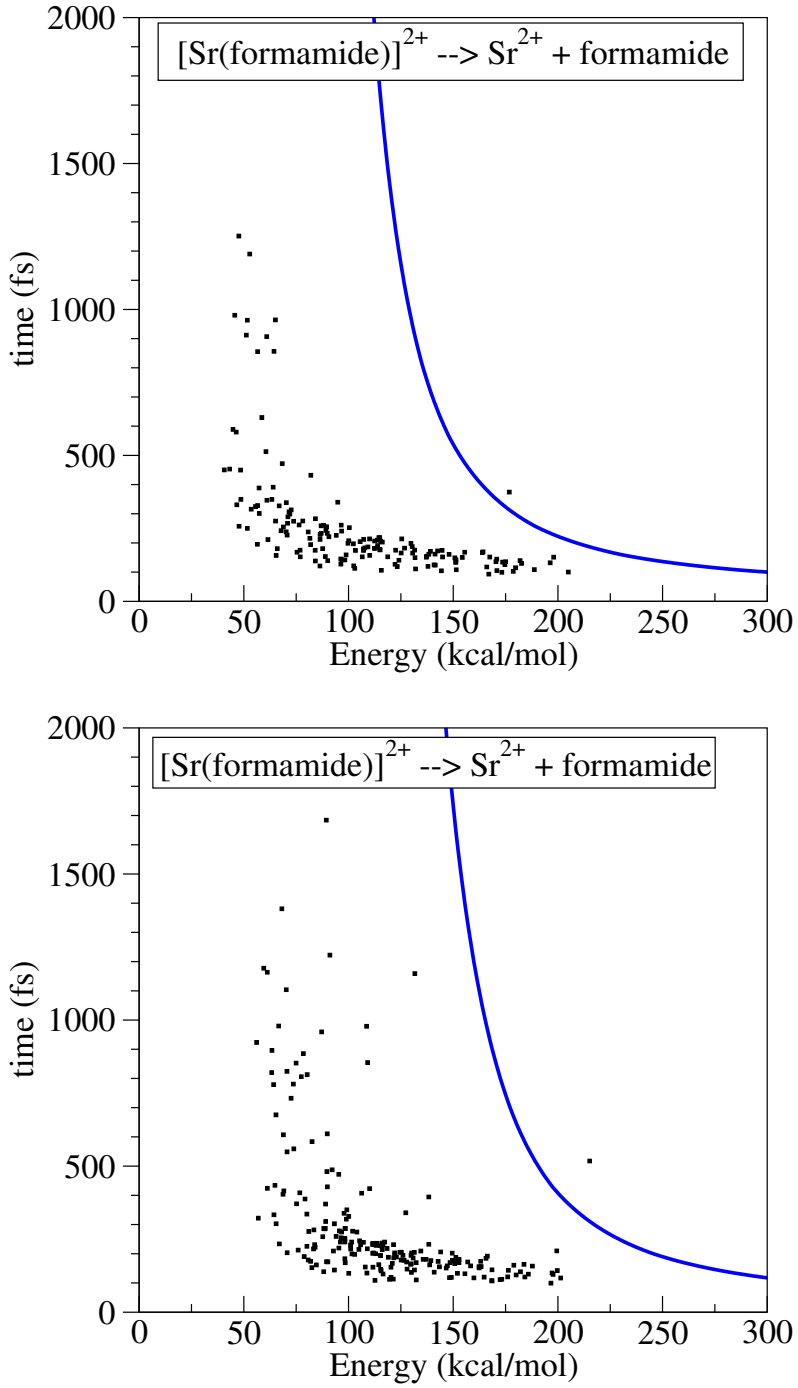

Figure S3: Reaction time *vs.* energy transfer obtained from dynamics simulations (squares) and half life times ($t_{1/2}$) predicted by RRKM (solid line). Both are for trajectories yielding formamide using G96LYP/6-31G(d) in the top and G96LYP/6-31+G(d,p) in the bottom.

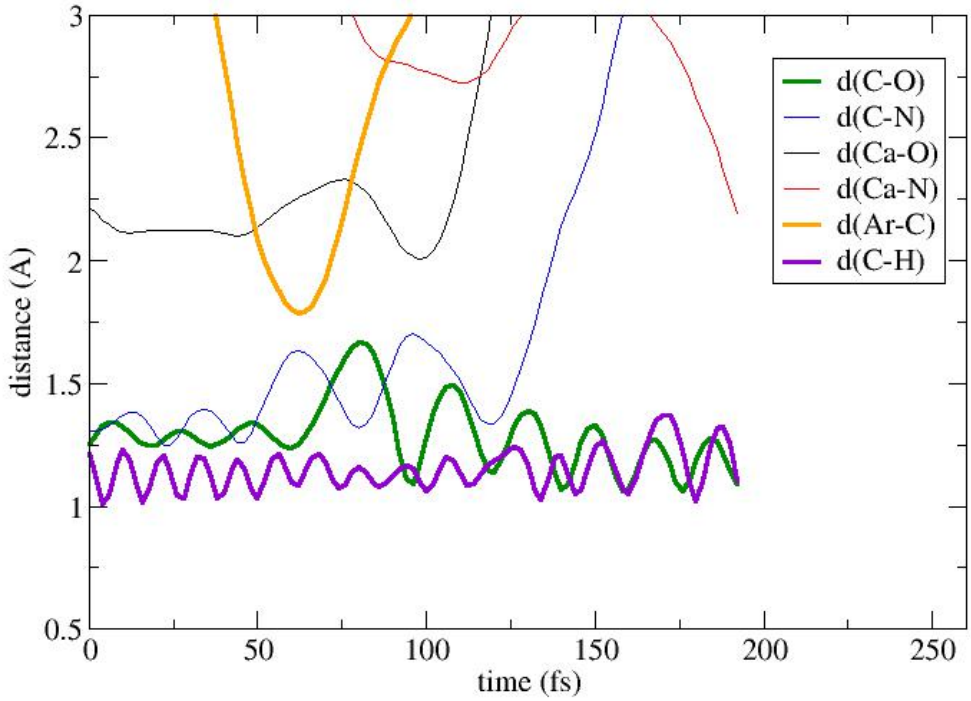

Figure S4. Selected distances for a trajectory yielding **G**, $[Ca(NH_2)]^+$ + HCO^+ Coulomb explosion (the same as Fig. 5a and video jp5076059_si_005.mpg). Distances already reported in Fig. 5a are shown as thin lines.

Before Ar approaches to the ion, C=O and C-H distances oscillate with a period of about 20 and 10 fs respectively, and an amplitude corresponding to n = 0 of their respective normal modes (1699 and 3075 cm^{-1}, for 20 and 10 fs) (these were extracted from equilibrium structure of $[Ca(formamide)]^{2+}$, min**1**). After the reaction, these bonds are found in the HCO^+ product, and their periods are of about 15 and 10 fs. Given the new amplitudes, and new frequencies (2173 (C=O) and 3181 cm^{-1} (C-H)), they correspond to n = 1 of both normal modes. Note that during the collision, *i.e.* when Ar is at a distance less then 3 Å, these vibrational modes do not correspond to the frequency of any reference structure (furthermore, no frequency can be identified). Hence, it is not possible to quantify them in terms of vibrational quantum states (or vibrational energies) during collision.

3.4. Efficiency of the energy transfer

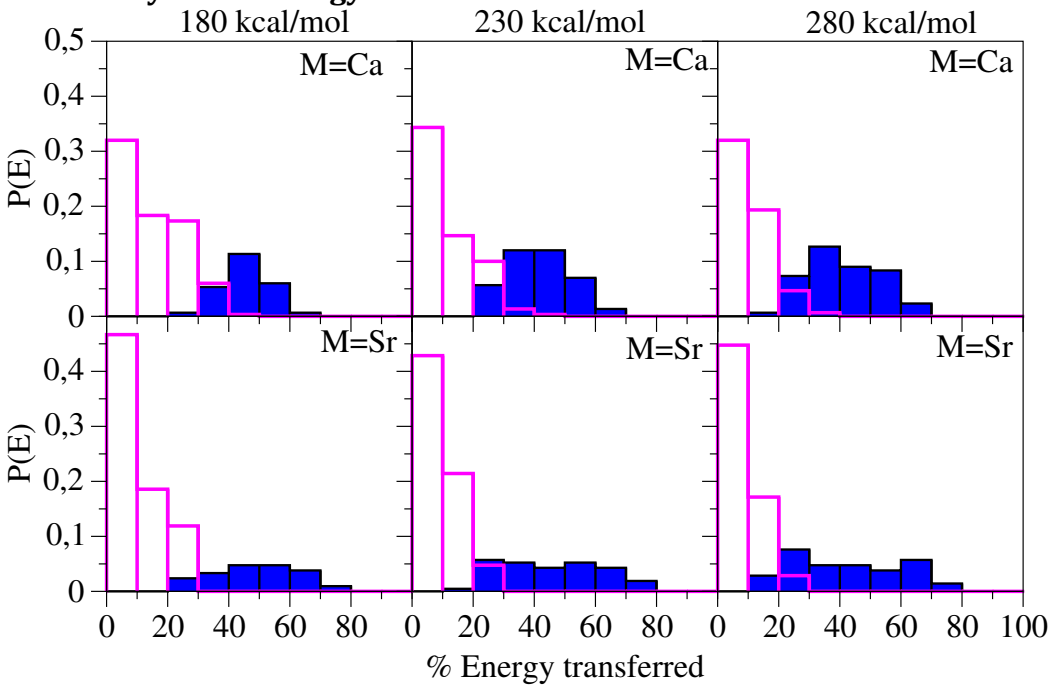

Figure S5: Probability of transferring a given % of the collision energy to the $[M(formamide)]^{2+}$ ion for the non-reactive trajectories (white) and the reactive ones (blue), at the three collision energies considered (180, 230 and 280 kcal mol^{-1} from left to right). G96LYP/6-31G(d) is used for the two molecular ions.

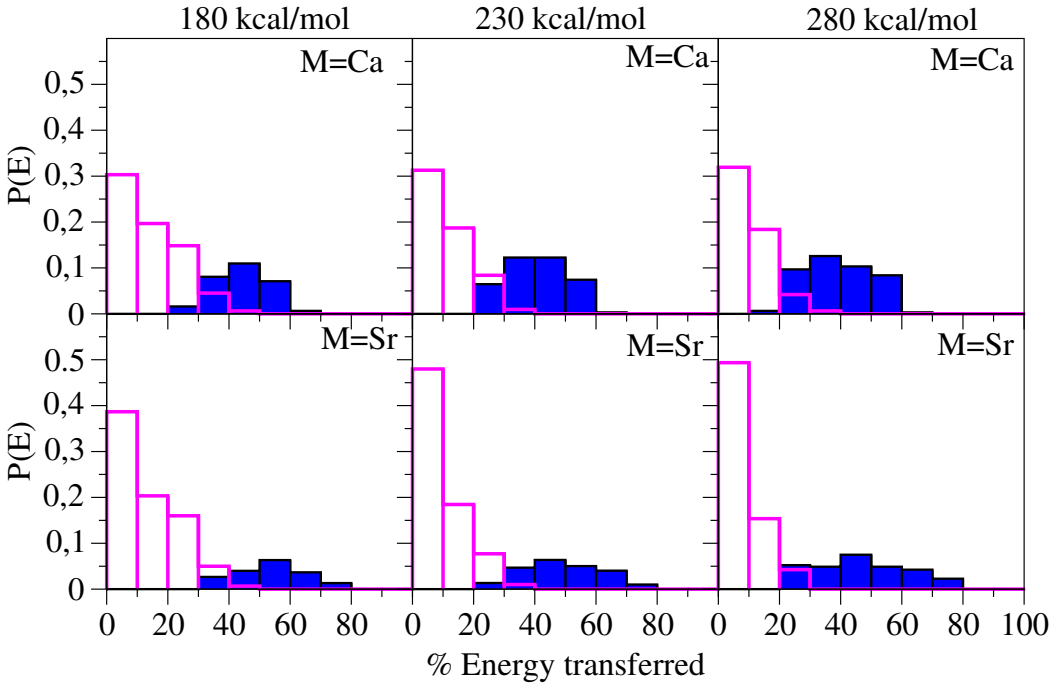

Figure S6: Probability of transferring a given % of the collision energy to the $[M(formamide)]^{2+}$ ion for the non-reactive trajectories (white) and the reactives ones (blue), at the three collision energies considered (180, 230 and 280 kcal mol^{-1} from left to right). The trajectories were calculated using BLYP/6-31G(d) for M = Ca and G96LYP/6-31+G(d,p) for M = Sr.

In general the profiles are quite similar for both system, with a somewhat smaller percentages of transferred energy for Sr containing system in the case of the non-reactive trajectories, but higher for the reactive ones. In all the cases the most probable events are small energy transfers (between 0-10kcal mol^{-1}). The probability of having a high percentage of energy transferred decreases progressively becoming zero for percentages higher than 70 % and 80% for Ca and Sr respectively. The reactive trajectories correspond to the highest amount of energy transferred, being the average for non-reactive about 13% and 44% for the reactive ones.

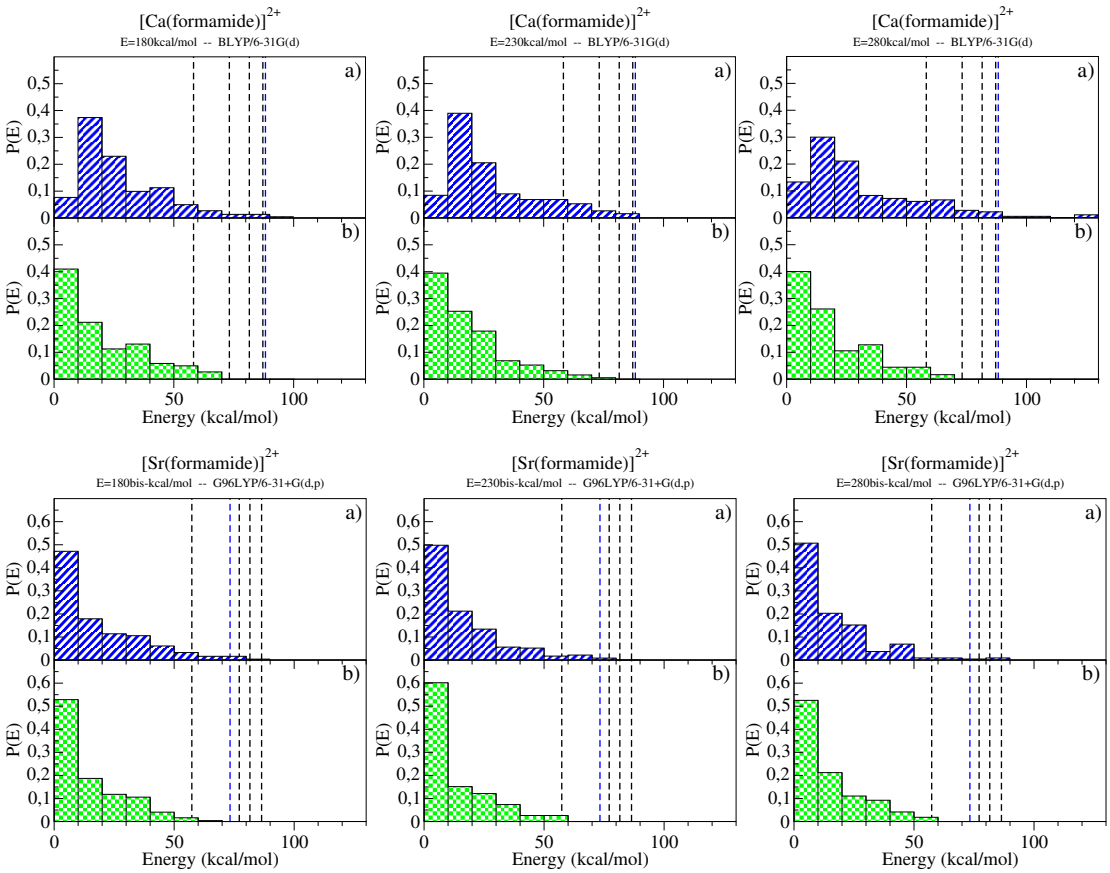

Figure S7: Vibrational (a panels) and rotational (b panels) energy distribution for the non-reactive trajectories at the three collision energies: 180, 230 and 280 kcal mol^{-1} from left to right. The top panels correspond to M = Ca while the bottom ones are for M = Sr. The dashed lines marked the energy for the different TS that can be reached from min**1** structure. The values for M = Ca are compute using the BLYP/6-31G(d) approach while the values for M = Sr are computed at the G96LYP/6-31+G(d,p) level of theory.

Scattering plots for [M(formamide)]$^{2+}$ (M = Ca, Sr)

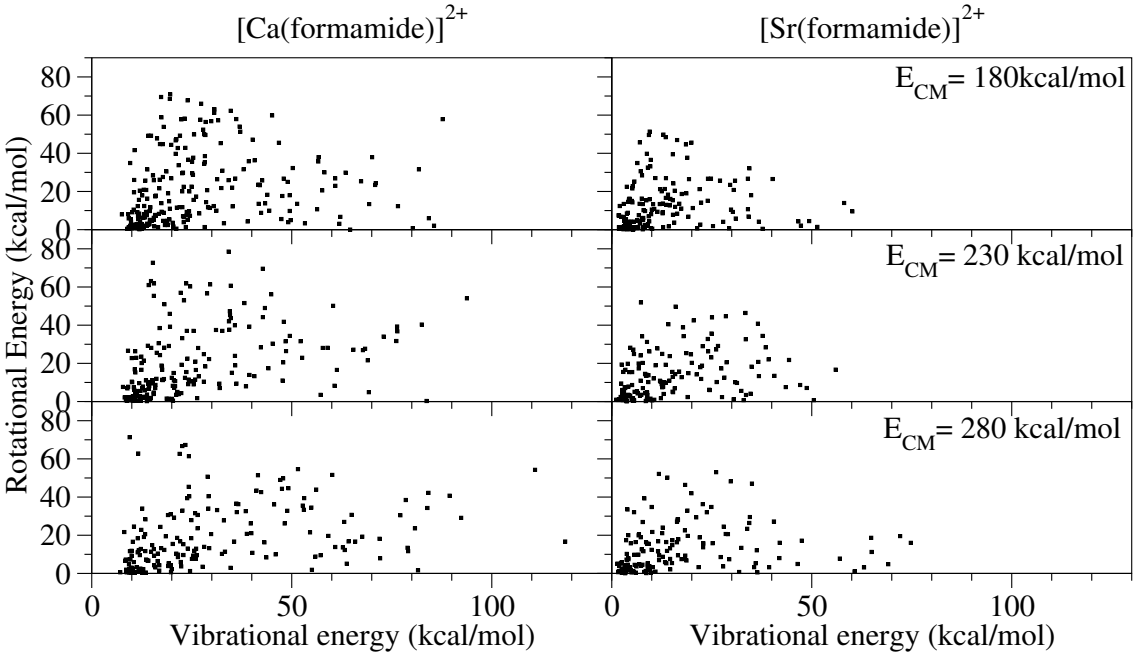

Figure S8: Scattering plot of vibrational versus rotational energy distributions obtained from nonreactive [M(formamide)]$^{2+}$ trajectories for the three collision energies considered. The level of theory used for both metals is: G96LYP/6-31G(d).

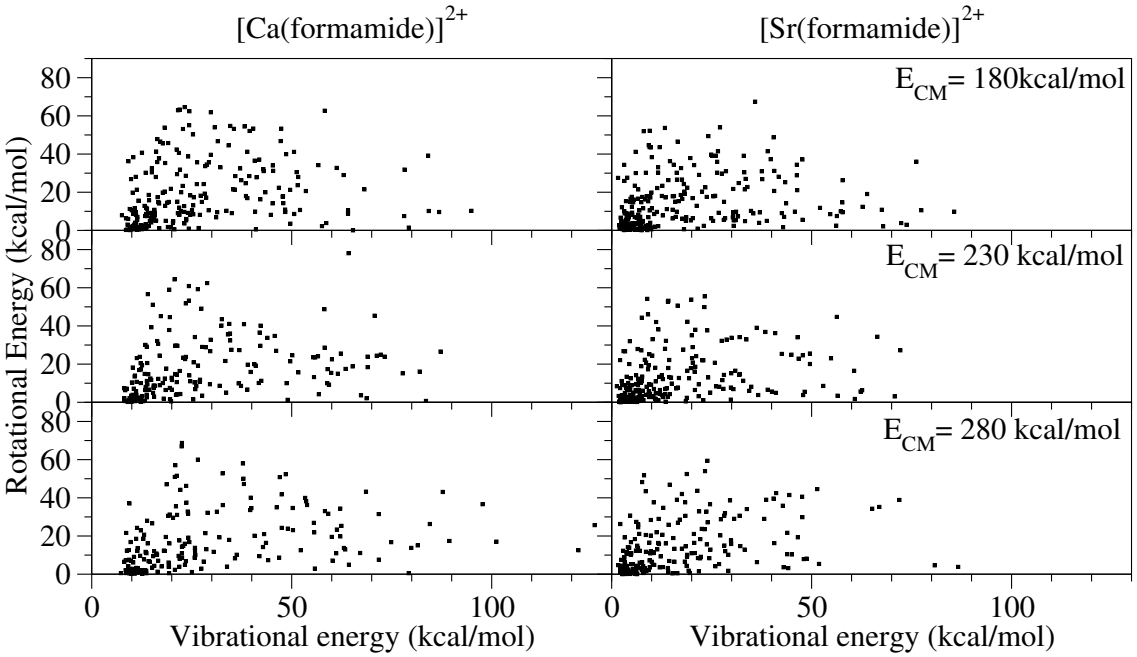

Figure S9: Scattering plot of vibrational versus rotational energy distributions obtained from nonreactive [M(formamide)]$^{2+}$ trajectories for the three collision energies. The trajectories were calculated using BLYP/6-31G(d) for M = Ca and G96LYP/6-31+G(d,p) for M = Sr.

Fig. S8 unambiguously show that vibrational excitation is independent from the rotational excitation. Similar results are obtained using BLYP/6-31G(d), M = Ca, and G96LYP/6-31+G(d,p), M = Sr, as shown in Fig. S9.

Kinetic analysis:

Harmonic frequencies (cm^{-1}) and energy threshold (kcal mol^{-1}) used to compute the RRKM constants shown in this work.

[Ca(formamide)]$^{2+}$

- k_1_2

Threshold: 58.00 kcal mol^{-1}
Harmonic frequencies (cm^{-1})
Reactant
3539.3,3435.5,3075.0,1699.8,1596.0,1387.9,1353.4, 1076.1,1028.4, 718.4, 668.8, 587.8, 361.3, 136.9, 127.8
TS
3446.0,3162.0,1970.3,1668.8,1287.0,1103.2,1055.2, 1012.5, 939.9, 828.0, 751.4, 322.6, 148.0, 110.1

- k_1_10

Threshold: 74.00 kcal mol^{-1}
Harmonic frequencies (cm^{-1})
Reactant
3539.3,3435.5,3075.0,1699.8,1596.0,1387.9,1353.4, 1076.1,1028.4, 718.4, 668.8, 587.8, 361.3, 136.9, 127.8
TS
3368.0,3292.6,3214.0,2068.4,1583.2, 899.8, 828.6, 768.7, 441.2, 405.2, 386.5, 173.6, 137.1, 32.5

- k_1_G

Threshold: 82.00 kcal mol^{-1}
Harmonic frequencies (cm^{-1})
Reactant
3539.3,3435.5,3075.0,1699.8,1596.0,1387.9,1353.4, 1076.1,1028.4, 718.4, 668.8, 587.8, 361.3, 136.9, 127.8
TS
3441.8,3362.3,3144.2,2061.3,1580.2, 598.9, 590.5, 562.6, 471.4, 425.9, 232.9, 111.6, 80.6, 21.8

- k_1_5

Threshold: 87.00 kcal mol^{-1}
Harmonic frequencies (cm^{-1})
Reactant
3539.3,3435.5,3075.0,1699.8,1596.0,1387.9,1353.4, 1076.1,1028.4, 718.4, 668.8, 587.8, 361.3, 136.9, 127.8
TS
3391.7,3166.7,1941.0,1577.7,1504.3,1312.0,1053.2, 1013.5, 800.1, 544.1, 515.0, 309.5, 115.9, 81.6

- k_2_1_rrkm

Threshold: 9.00 kcal mol^{-1}
Harmonic frequencies (cm^{-1})
Reactant
3436.3,3371.9,3098.4,1749.4,1331.7,1255.2,1019.0, 938.3, 798.1, 720.2, 634.8, 595.9, 287.5, 137.5, 66.1
TS
3446.0,3162.0,1970.3,1668.8,1287.0,1103.2,1055.2, 1012.5, 939.9, 828.0, 751.4, 322.6, 148.0, 110.1

- k_2_A_rrkm

Threshold: 7.00 kcal mol^{-1}
Harmonic frequencies (cm^{-1})
Reactant
3436.3,3371.9,3098.4,1749.4,1331.7,1255.2,1019.0, 938.3, 798.1, 720.2, 634.8, 595.9, 287.5, 137.5, 66.1
TS
3667.9,3588.7,3218.7,2024.4,1141.1,1028.3, 796.1, 616.6, 544.9, 441.3, 388.3, 228.2, 124.3, 42.7

- k_2_3_rrkm

Threshold: 2.00 kcal mol^{-1}
Harmonic frequencies (cm^{-1})
Reactant
3436.3,3371.9,3098.4,1749.4,1331.7,1255.2,1019.0, 938.3, 798.1, 720.2, 634.8, 595.9, 287.5, 137.5, 66.1
TS
3513.3,3400.9,3104.9,1724.1,1291.6,1255.2,1043.0, 968.9, 814.0, 682.2, 600.2, 364.9, 310.2, 148.0

- k_3_2_rrkm

Threshold: 33.00 kcal mol^{-1}
Harmonic frequencies (cm^{-1})
Reactant
3558.1,3435.8,3117.3,1653.5,1378.3,1279.1,1191.9, 1048.6, 997.6, 828.7, 707.9, 478.8, 337.4, 275.1, 178.4
TS
3513.3,3400.9,3104.9,1724.1,1291.6,1255.2,1043.0, 968.9, 814.0, 682.2, 600.2, 364.9, 310.2, 148.0

- k_10_11_rrkm

Threshold: 0.00 kcal mol^{-1}
Harmonic frequencies (cm^{-1})
Reactant
3375.2,3327.5,3108.4,2176.8,1701.7,1672.2,1454.4, 744.4, 660.6, 374.8, 300.9, 159.5, 134.3, 134.2, 49.6
TS
3384.1,3345.7,3229.9,2174.6,1685.2,1668.7,1408.4, 690.2, 639.1, 370.9, 235.4, 127.6, 123.3, 109.8

- k_10_1_rrkm

Threshold: 45.00 kcal mol^{-1}
Harmonic frequencies (cm^{-1})
Reactant
3375.2,3327.5,3108.4,2176.8,1701.7,1672.2,1454.4, 744.4, 660.6, 374.8, 300.9, 159.5, 134.3, 134.2, 49.6
TS
3368.0,3292.6,3214.0,2068.4,1583.2, 899.8, 828.6, 768.7, 441.2, 405.2, 386.5, 173.6, 137.1, 32.5

- k_11_10

Threshold: 16.00 kcal mol^{-1}
Harmonic frequencies (cm^{-1})
Reactant
3378.0,3378.0,3302.4,2220.8,1676.1,1675.8,1422.6, 621.5, 620.7, 354.8, 211.1, 211.1, 196.7, 17.9, 16.8
TS
3384.1,3345.7,3229.9,2174.6,1685.2,1668.7,1408.4, 690.2, 639.1, 370.9, 235.4, 127.6, 123.3, 109.8

[Sr(formamide)]$^{2+}$

- k_1_2

Threshold: 54.00 kcal mol^{-1}
Harmonic frequencies (cm^{-1})
Reactant
3557.6,3450.1,3043.6,1709.5,1608.7,1392.4,1341.3,1070.1,1030.0, 705.8, 618.4, 576.4, 257.4, 125.6, 116.1
TS
3459.1,3157.6,1993.7,1657.5,1309.2,1123.1,1086.9, 1041.0, 952.2, 840.0, 727.4, 226.3, 129.7, 102.5

- k_1_10

Threshold: 76.00 kcal mol^{-1}
Harmonic frequencies (cm^{-1})
Reactant
3557.6,3450.1,3043.6,1709.5,1608.7,1392.4,1341.3, 1070.1,1030.0, 705.8, 618.4, 576.4, 257.4, 125.6, 116.1
TS
3374.6,3301.3,3212.5,2038.9,1603.3, 912.7, 877.8, 784.1, 445.8, 410.7, 366.4, 168.6, 135.9, 33.1

- k_1_G

Threshold: 88.16 kcal mol^{-1}
Harmonic frequencies (cm^{-1})
Reactant
3557.6,3450.1,3043.6,1709.5,1608.7,1392.4,1341.3, 1070.1,1030.0, 705.8, 618.4, 576.4, 257.4, 125.6, 116.1
TS
3461.2,3385.8,3050.4,2025.3,1609.9,659.0,521.8, 502.1, 410.3, 399.8, 208.1, 108.8, 71.0, 19.8

- k_1_5

Threshold: 86.00 kcal mol^{-1}
Harmonic frequencies (cm^{-1})
Reactant
3557.6,3450.1,3043.6,1709.5,1608.7,1392.4,1341.3, 1070.1,1030.0, 705.8, 618.4, 576.4, 257.4, 125.6, 116.1
TS
3406.2,3178.3,1939.7,1572.0,1548.2,1306.7,1035.5, 984.1, 752.2, 524.4, 488.8, 232.6, 104.7, 74.8

Table S1: Values of the RRKM rate constants, k(s^{-1}), for some selected energies, E (kcal mol^{-1}). Rate constants adding one third of the total rotational energy, E_T(rot), to each of the rotational axis are marked with an asterisk, k*.

a) M = Ca. E_T(rot)= 27 kcal mol^{-1}

E	k_{01}	k_{01}*	k_{12}	k_{110}	k_{110}*	k_{1G}	k_{1G}*	k_{15}
45	---	---	---	---	---	---	---	---
55	$2.70\cdot10^{5}$	---	---	---	---	---	---	---
65	$1.16\cdot10^{8}$	---	$1.90\cdot10^{6}$	---	---	---	---	---
75	$1.65\cdot10^{9}$	$3.98\cdot10^{6}$	$7.22\cdot10^{7}$	$1.75\cdot10^{4}$	---	---	---	---
85	$8.76\cdot10^{9}$	$5.02\cdot10^{8}$	$6.29\cdot10^{8}$	$3.38\cdot10^{7}$	---	$3.99\cdot10^{5}$	---	---
95	$2.81\cdot10^{10}$	$5.10\cdot10^{9}$	$2.85\cdot10^{9}$	$9.04\cdot10^{8}$	$1.18\cdot10^{5}$	$2.66\cdot10^{8}$	$1.20\cdot10^{6}$	$1.74\cdot10^{5}$
105	$6.68\cdot10^{10}$	$2.20\cdot10^{10}$	$8.82\cdot10^{9}$	$7.51\cdot10^{9}$	$1.17\cdot10^{8}$	$6.59\cdot10^{9}$	$1.39\cdot10^{9}$	$8.26\cdot10^{6}$
115	$1.32\cdot10^{11}$	$6.21\cdot10^{10}$	$2.14\cdot10^{10}$	$3.47\cdot10^{10}$	$2.61\cdot10^{9}$	$5.54\cdot10^{10}$	$3.39\cdot10^{10}$	$9.26\cdot10^{7}$
125	$2.29\cdot10^{11}$	$1.37\cdot10^{11}$	$4.38\cdot10^{10}$	$1.12\cdot10^{11}$	$1.94\cdot10^{10}$	$2.63\cdot10^{11}$	$2.64\cdot10^{11}$	$5.26\cdot10^{8}$

b) M = Sr. E_T(rot)= 18 kcal mol^{-1}

E	k_{01}	k_{01}*	k_{12}	k_{110}	k_{110}*	k_{1G}	k_{1G}*	k_{15}
45	$6.19\cdot10^{5}$	---	---	---	---	---	---	---
55	$2.98\cdot10^{8}$	---	$3.24\cdot10^{4}$	---	---	---	---	---
65	$3.80\cdot10^{9}$	$4.71\cdot10^{8}$	$1.72\cdot10^{7}$	---	---	---	---	---
75	$1.84\cdot10^{10}$	$6.70\cdot10^{9}$	$2.85\cdot10^{8}$	---	---	---	---	---
85	$5.60\cdot10^{10}$	$3.18\cdot10^{10}$	$1.73\cdot10^{9}$	$5.65\cdot10^{6}$	---	---	---	---
95	$1.28\cdot10^{11}$	$9.24\cdot10^{10}$	$6.31\cdot10^{9}$	$2.27\cdot10^{8}$	$1.33\cdot10^{6}$	$4.73\cdot10^{6}$	---	$5.84\cdot10^{5}$
105	$2.40\cdot10^{11}$	$2.00\cdot10^{11}$	$1.69\cdot10^{10}$	$2.25\cdot10^{9}$	$1.39\cdot10^{8}$	$5.56\cdot10^{8}$	$8.62\cdot10^{7}$	$2.31\cdot10^{7}$
115	$3.96\cdot10^{11}$	$3.66\cdot10^{11}$	$3.69\cdot10^{10}$	$1.15\cdot10^{10}$	$1.88\cdot10^{9}$	$8.90\cdot10^{9}$	$4.28\cdot10^{9}$	$2.40\cdot10^{8}$
125	$5.99\cdot10^{11}$	$5.89\cdot10^{11}$	$6.98\cdot10^{10}$	$3.98\cdot10^{10}$	$1.12\cdot10^{10}$	$6.13\cdot10^{10}$	$4.75\cdot10^{10}$	$1.30\cdot10^{9}$

Intermediate 2 from [Ca(formamide)]$^{2+}$ and from [Sr(formamide)]$^{2+}$:

The upper part of Fig. S10 shows the corresponding kinetic schemes for both metal ions. In the bottom part are represented the RRKM rate constants for the matching reactions.

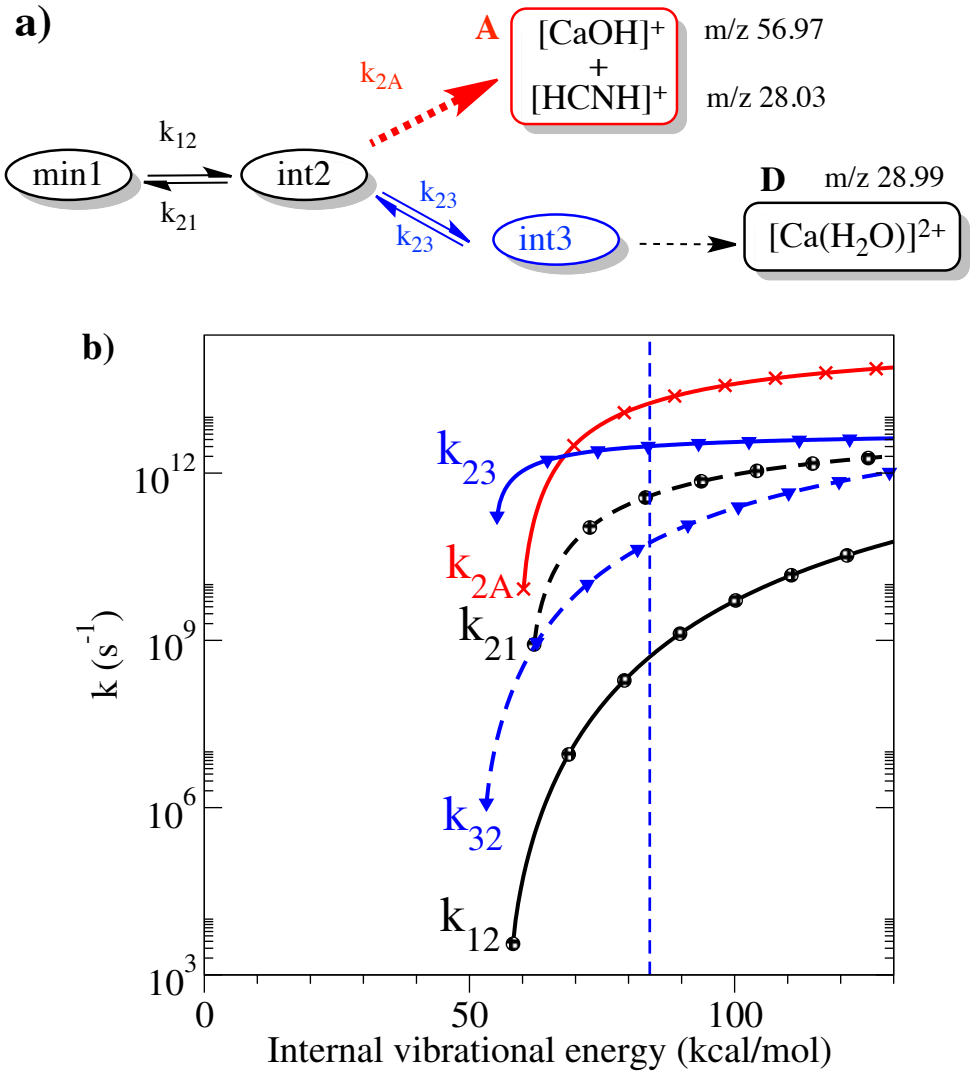

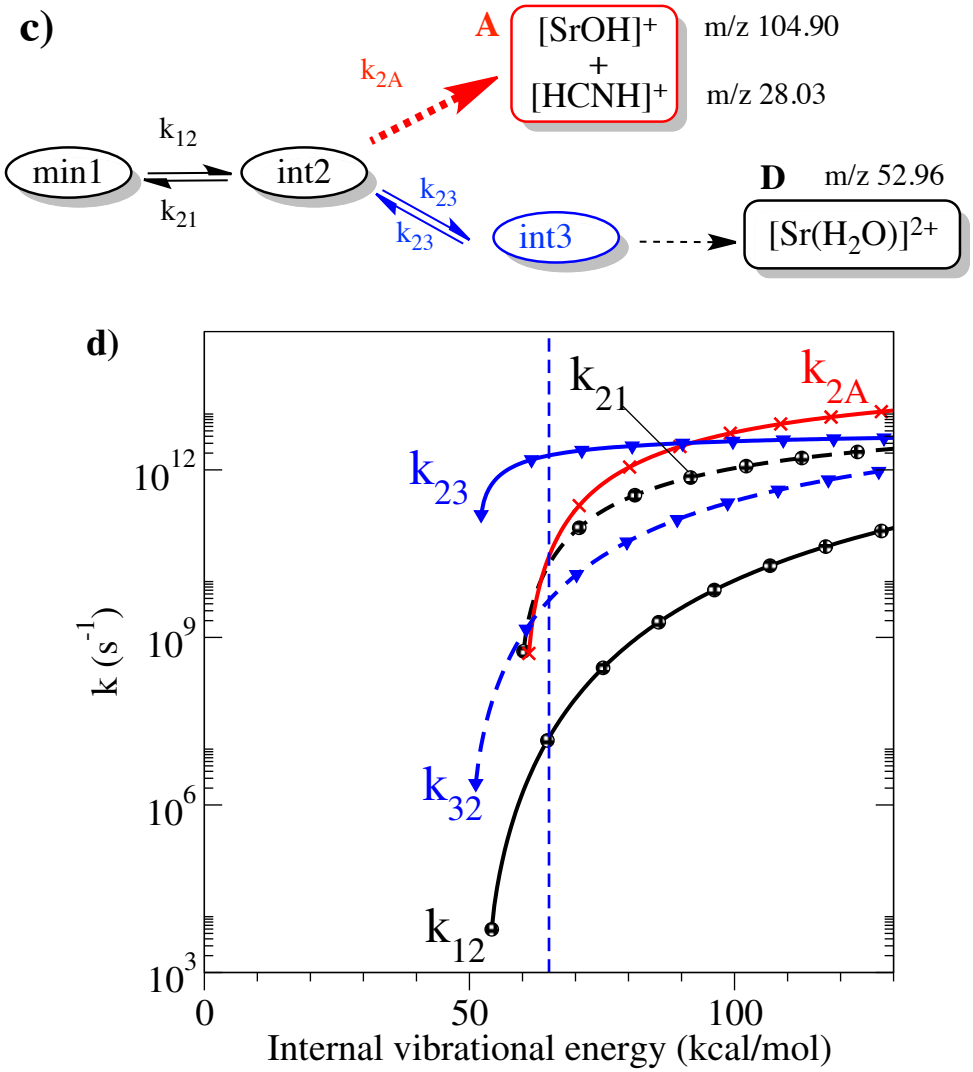

Figure S10: Upper part: kinetic scheme for the reactions that can take place starting from int**2**, **a)** M = Ca, **c)** M = Sr. In the bottom part are shown the corresponding RRKM rate constants.

From int**2** there are three possible options: going back to the origin, min**1**; fragmentation of int**2** via Coulomb explosion into products **A**, and an isomerization to int**3** that would eventually loose ammonia to provide product **D**. For the sake of consistency, the curves were shifted to the left of a quantity corresponding to the relative energy of each intermediate with respect to min**1**. The first conspicuous observation is that for both Ca and Sr the backward reaction to min**1** (k_{21}) is faster than the forward one (k_{12}); but reactions towards int**3** (k_{23}) and products **A** are even faster. There are, however, some subtle differences between the two metals as far as the reaction to **A** products is concerned. Whereas for M = Ca this reaction is much faster than the one going back to min**1** and that yielding int**3**, for M = Sr it is slower than k_{23} and competes with k_{21}. Thus, for M = Ca, int**2** would rapidly evolve to products **A** and a very small fraction would isomerize to int**3**, whereas for M = Sr most of the flux will follow the path leading to int**3**. In both cases this intermediate will eventually evolve to product **D**: $[M(H_2O)]^{2+}$ (M = Ca, Sr).
Similar analyses have been performed for the intermediate int**10** that eventually yields product **B**: $[Ca(NH_3)]^{2+}$ (see Fig. S11).

Intermediate 10 from [Ca(formamide)]$^{2+}$:

In the case of [Ca(formamide)]$^{2+}$ ion, a small fraction of the non-reactive ions has energy enough to follow the path leading to int**10**. This intermediate has two possible ways to evolve (see Fig. S11): either it comes back to min**1** or it evolves to form product **B**. In this case, int**10** → min**1** backward reaction is slower than the forward, so once int**10** is formed it will not interconvert back to products. From int**10** there are two possible pathways to follow. A direct path from int**10** to **B** or a path passing trough int**11**, which can also evolve to product **B**. Between these two options the fastest is forming **B** directly from int**10**. Therefore, most of the flux will follow this path.

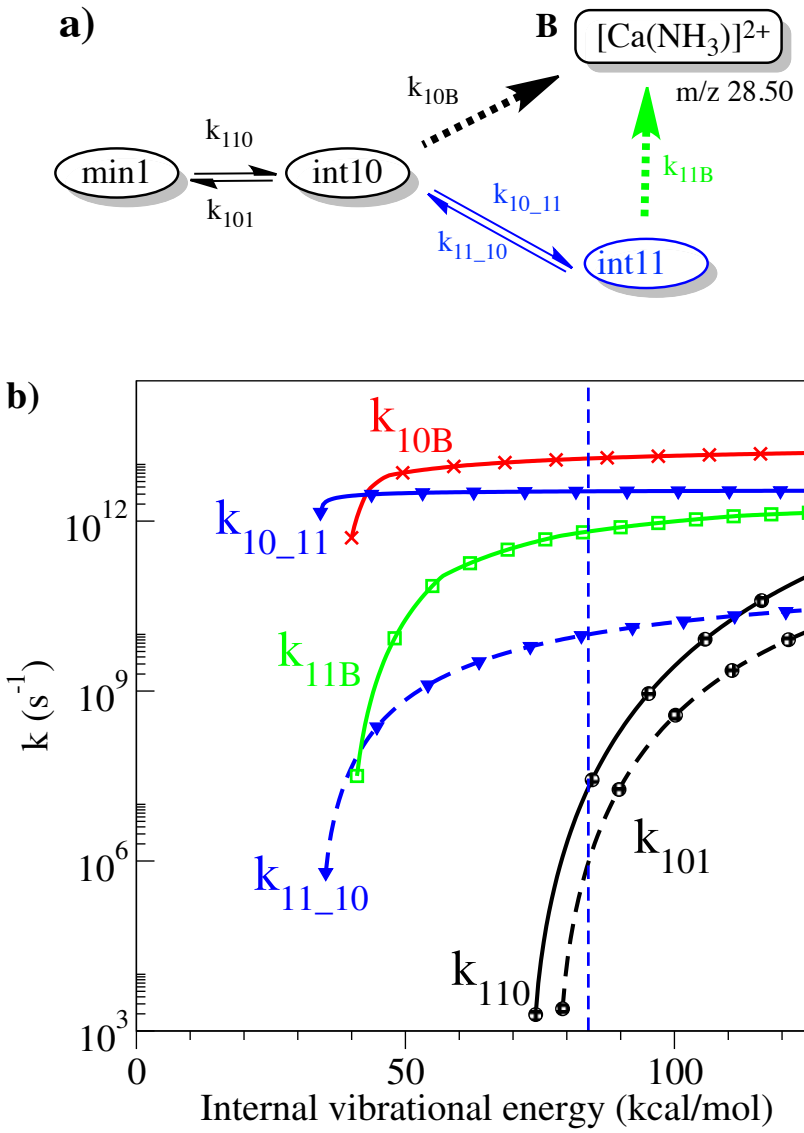

Figure S11: a) kinetic scheme for the reactions that can take place starting from int**10**, **b)** corresponding RRKM rate constants, with (green lines) and without (black lines) rotational energy.